

Permeation and Block by Internal and External Divalent Cations of the Catfish Cone Photoreceptor cGMP-gated Channel

LAWRENCE W. HAYNES

From the Department of Medical Physiology, the Neuroscience Research Group and Lions' Sight Centre, University of Calgary, Calgary, Alberta, T2N 4N1, Canada

ABSTRACT The ability of the divalent cations calcium, magnesium, and barium to permeate through the cGMP-gated channel of catfish cone outer segments was examined by measuring permeability and conductance ratios under biionic conditions and by measuring their ability to block current carried by sodium when presented on the cytoplasmic or extracellular side of the channel. Current carried by divalent cations in the absence of monovalent cations showed the typical rectification pattern observed from these channels under physiological conditions (an exponential increase in current at both positive and negative voltages). With calcium as the reference ion, the relative permeabilities were $\text{Ca} > \text{Ba} > \text{Mg}$, and the chord conductance ratios at +50 mV were in the order of $\text{Ca} \approx \text{Mg} > \text{Ba}$. With external sodium as the reference ion, the relative permeabilities were $\text{Ca} > \text{Mg} > \text{Ba} > \text{Na}$ with chord conductance ratios at +30 mV in the order of $\text{Na} \gg \text{Ca} = \text{Mg} > \text{Ba}$. The ability of divalent cations presented on the intracellular side to block the sodium current was in the order $\text{Ca} > \text{Mg} > \text{Ba}$ at +30 mV and $\text{Ca} > \text{Ba} > \text{Mg}$ at -30 mV. Block by external divalent cations was also investigated. The current-voltage relations showing block by internal divalent cations reveal no anomalous mole fraction behavior, suggesting little ion-ion interaction within the pore. An Eyring rate theory model with two barriers and a single binding site is sufficient to explain both these observations and those for monovalent cations, predicting a single-channel conductance under physiological conditions of 2 pS and an inward current at -30 mV carried by 82% Na, 5% Mg, and 13% Ca.

• INTRODUCTION

The cGMP-gated channels of rod and cone photoreceptors are nonspecific cation channels that pass both monovalent and divalent cations (Furman and Tanaka, 1990; Menini, 1990; Colamartino, Menini, and Torre, 1991; Zimmerman and Baylor, 1992; Picones and Korenbrot, 1992; Haynes, 1994, 1995). While the selectivity of rod and cone channels for monovalent cations is not very different, there is rea-

Address correspondence to Dr. L. W. Haynes, Department of Medical Physiology, University of Calgary, 3330 Hospital Drive NW, Calgary, Alberta T2N 4N1, Canada.

son to expect that the cone channel passes more divalent current than the rod channel. In the absence of divalent cations (Yau and Haynes, 1986), the channels of both rods (Haynes, Kay, and Yau, 1986; Zimmerman and Baylor, 1986) and cones (Haynes and Yau, 1990*a*) are unblocked and the current-voltage relations retain only a slight outward rectification. Under physiological conditions, the current-voltage relations obtained are quite different for channels from rods or from cones (cf. Fig. 1 of Haynes and Yau, 1990*b*). Over the voltage range of ± 60 mV, the current through the rod channel strongly rectifies in the outward direction (Fesenko, Kolesnikov, and Lyubarsky, 1985; Yau, Haynes, and Nakatani, 1986) such that the current at positive potentials increases exponentially while the current at negative potentials is nearly constant. The current through the cone channel under identical conditions, on the other hand, increases exponentially at both positive and negative potentials (Haynes and Yau, 1985). In both types of channels, this rectification is due to voltage-dependent block of the Na current by permeant divalent cations, primarily Ca^{2+} and Mg^{2+} . In the presence of divalent cations, the increase in current at negative potentials through the cone channels must be due to a relief of block. The simplest mechanism by which this could come about is if the rate of permeation of the blocking ions increased at negative potentials (i.e., decreased strength of block). This would suggest (Haynes, 1991) that the ratio of divalent and monovalent current is greater in the cone channel than in the rod channel. Experiments by Perry and McNaughton (1991) measuring the dark current and calcium loading of cones have concluded that the fraction of the dark current carried by calcium entering a cone is indeed twice that of the rod. Because calcium is known to play a crucial role in light adaptation (Matthews, Murphy, Fain, and Lamb, 1988; Nakatani and Yau, 1988*a*) and the control of cGMP levels (e.g., Koch and Stryer, 1988), this higher permeability may have profound consequences for the rate of light adaptation in the cone.

In the previous paper, I examined the permeation of monovalent cations through the cGMP-gated channel of catfish cones (Haynes, 1995). This study extends that investigation to characterize the permeation of the divalent cations calcium, magnesium, and barium and will show that the relative permeabilities of these ions are greater than that of sodium, but that their relative conductances are lower. These results are summarized in a model of ion permeation using Eyring rate theory.

This work has previously been described briefly in abstract form (Haynes, 1991, 1993, 1994).

METHODS

The general methods, including correction for liquid junction potentials, leak subtraction, the construction of Eyring rate theory models, et cetera, have been described in the previous paper (Haynes, 1995). Only methods specific to experiments using divalent cations are described here.

Solutions

A number of different solutions were used in these experiments. For solutions containing divalent cations alone, each solution contained the chloride salt of the divalent cation together with 5 mM of the divalent cation salt of HEPES (pH 7.6). Mixtures of divalent and monovalent cations were made by the addition of the divalent cation chloride salt to the monovalent cation solution in the

absence of chelators. Since the concentration of divalent cations was usually large, and always larger than the level of contaminating divalent cations in the monovalent cation solution, buffering with EGTA was deemed unnecessary. In some experiments, the solution filling the pipette was replaced by perfusing the interior of the pipette using the 2PK+ pipette perfusion system (Adams and List, Westbury, NY). A fine quartz canula was inserted down the length of the pipette and attached to a pressure vessel filled with the perfusing solution. Because patches excised from cones are relatively fragile, application of a vacuum to the pipette holder to initiate perfusion was not used. Instead, positive pressure was applied to the vessel containing the perfusate when required, causing solution flow through the cannula. Several minutes were required before replacement of the solution at the tip of the pipette was complete.

The activity coefficients of the monovalent and divalent cations were calculated using the parametric equations of Pitzer and Mayorga (1973) and the activity of a divalent cation is given according to the Guggenheim convention. The Harned rule for correcting ion activities in mixed solutions was not used since the correction coefficient was available only for calcium (Butler, 1968). Failure to apply the Harned rule results in <1% overestimation of the calcium concentration and, presumably, the other divalent cations. Molarity and molality conversion was performed according to the formulas in Robinson and Stokes (1970). For convenience, all references to concentration in this paper are to the concentration of the solution as mixed. The actual ion activity is given in the text where appropriate and is used in all calculations.

Data Analysis

The permeability ratio of divalent cation X^{2+} at the intracellular surface with respect to monovalent cation Y^+ at the extracellular surface can be obtained by solving the Goldman-Hodgkin-Katz current equation (see Lewis, 1979, Appendix I), resulting in

$$\frac{P_{X^{2+}}}{P_{Y^+}} = \frac{[Y^+]_o}{4[X^{2+}]_i} \left(e^{\frac{-F\Delta V_{Rev}}{RT}} + e^{\frac{FDV_{Rev}}{RT}} \right) \quad (1)$$

where P_X/P_Y is the permeability ratio of divalent ion X with respect to monovalent ion Y , V_{Rev} is the change in reversal potential, the subscripts i and o refer to the cytoplasmic and extracellular surfaces of the patch, respectively, and R , T , and F have their usual thermodynamic meaning. If identical concentrations of a monovalent cation are present on both sides of a patch and the divalent cation is present on only one side of the patch, two other solutions to the GHK equation are obtained. For divalent cations on the intracellular side, one obtains

$$\frac{P_{X^{2+}}}{P_{Y^+}} = \frac{[Y^+]}{4[X^{2+}]_i} \left(e^{-\frac{2F\Delta V_{Rev}}{RT}} - 1 \right) \quad (2)$$

and for divalent cations present on the extracellular side of the patch, one obtains

$$\frac{P_{X^{2+}}}{P_{Y^+}} = \frac{[Y^+]}{4[X^{2+}]_o} \left(e^{\frac{2F\Delta V_{Rev}}{RT}} - 1 \right). \quad (3)$$

Conductances were measured at a fixed membrane potential to avoid any possible effects of voltage-dependent gating. All conductances were chord conductances, determined by dividing the current at a given voltage by the driving force.

Throughout, data are presented as mean \pm SD. All statistical tests use the Student's t test.

RESULTS

Permeability and Conductance of Divalent Cations

Permeability and conductance ratios were determined for Ca, Mg, and Ba under bi-ionic conditions with Ca as the extracellular cation. These experiments were extremely difficult to perform successfully for two reasons. First, calcium promotes sealing of the patch into a vesicle upon excision. Second, the very small unitary conductance of the channel under these conditions means that patches with a large number of channels must be obtained. As a result, only five such experiments could be completed. One benefit of the high concentration of divalent cations, however, was very tight seals ($>100\text{ G}\Omega$) of exceptional stability which made resolving these small currents much easier. Data from one such experiment are shown in Fig. 1. In this experiment, 80 mM Mg (24 mM activity) and 80 mM Ba (22 mM activity) were tested against 40 mM Ca (14 mM activity). The reversal potentials were all near zero. Because there was a twofold difference in concentration between calcium and the other ions, the order of the permeability ratios is $\text{Ca} > \text{Ba} > \text{Mg}$. The mean permeability ratios for Ca:Ba:Mg were 1.0 ($n = 5$), 0.78 ± 0.14 ($n = 2$) and 0.59 ± 0.14 ($n = 5$). The average chord conductance ratios at +50 mV were in the order $\text{Ca} \approx \text{Mg} > \text{Ba}$ ($1.0:0.94 \pm 0.52:0.09 \pm 0.03$). Calcium is probably a better carrier of current than this measure would indicate, because its concentration is only

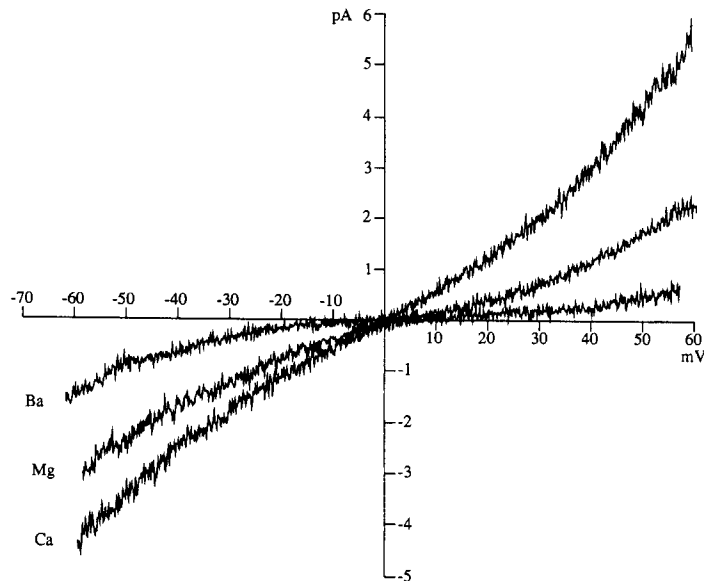


FIGURE 1. Current-voltage relation for divalent cations under bi-ionic conditions. Ca, Mg, or Ba was present on the cytoplasmic side of the patch with activities of 14, 24, and 22 mM, respectively, and Ca was present on the extracellular side at an activity of 14 mM. The reversal potentials for Ca, Mg and Ba were 0, +2.9, and 0 mV, giving permeability ratios of 1:0.51:0.69. The conductance ratios at +60 mV were 1.0, 0.42, and 0.1, respectively.

half that of the other ions. It should also be noted that recovery from exposure to barium was often incomplete, for reasons that are not clear.

The permeability and conductance ratios of Ca, Ba, and Mg with respect to extracellular Na under biionic conditions were also determined (Fig. 2). Because the divalent cations carry so little current, correction for the leakage current can be difficult. Indeed, the measured permeability ratios were highly variable, which might at first be taken to indicate that these values are unreliable. This variability, however, is seen from different patches during the course of a day's experiments and far exceeds the variability seen under similar experimental conditions with monovalent cations (Haynes, 1995). This and later experiments suggest that this variability may be physiologically significant. Only those experiments where the current carried by divalent cations clearly exceeded that of the leakage current and where the leakage

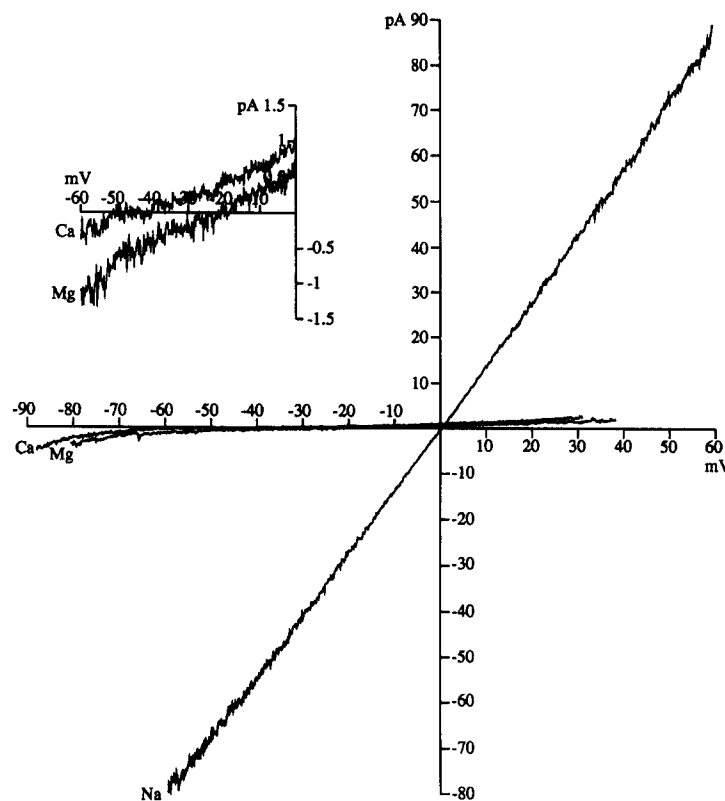


FIGURE 2. Current-voltage relation for divalent cations vs sodium under biionic conditions. 120 mM Na or 80 mM Ca or Mg were present on the cytoplasmic side of the patch (activities of 92, 23, and 24 mM, respectively), and 120 mM Na (92 mM activity) was present on the extracellular side. The reversal potentials for Na, Ca, and Mg were 0, -44 , and -19 mV, giving permeability ratios of 1:36:6. The conductance ratios at $+30$ mV were 1.0, 0.022, and 0.021, respectively. The inset shows the current-voltage relations with Ca and Mg at a 20-fold higher gain. Only portions of the currents in Ca and Mg near their reversal potentials are shown.

current in the second determination was the same as in the first determination were used. In all cases, the currents in the presence of divalent cations were recorded at a higher gain (typically 5- to 10-fold higher) to facilitate analysis. From the relative flatness of the current-voltage relation at positive potentials in Fig. 2, one might expect that determining the reversal potential would be difficult, but this flatness is an artifact of compressing the vertical scale of the small currents. The currents, in fact, increased exponentially with voltage at both positive and negative potentials, yielding easily identifiable reversal potentials (see Fig. 2, *inset*). When tested against 120 mM sodium, 80 mM concentrations of all three divalent cations produced strongly negative reversal potentials, indicating that the divalent cations all had greater permeability than sodium. The permeability ratios were in the order $\text{Ca} > \text{Ba} > \text{Mg} > \text{Na}$ in the ratio of 87 ± 63 ($n = 9$): 26 ± 15 ($n = 3$): 14 ± 11 ($n = 3$):1 ($n = 10$). All of the divalent cations had much lower conductances than sodium. The chord conductance ratios at +30 mV were in the order $\text{Na} \gg \text{Ca} = \text{Mg} > \text{Ba}$ ($1:0.016 \pm 0.007:0.016 \pm 0.005:0.012 \pm 0.006$).

Block of Sodium Current by Divalent Cations from the Internal Side

The low conductance supported by divalent cations suggests that information about the location and depth of the ion binding site might be obtained by treating the divalent cation as an (effectively) impermeant blocker of the sodium current. As an example, block of the sodium current by calcium is shown in Fig. 3. Very similar results were obtained for magnesium and barium. When divalent cations (0–6.4 mM) were added to the solution bathing the cytoplasmic side of the patch, the outward current was blocked to a greater degree than the inward current, resulting in an inward rectification of the current-voltage relation. At the higher concentrations, there was always a small shift in the reversal potential toward more negative values. As with the biionic sodium-calcium experiments, this again suggests a permeability ratio >1 for Ca with respect to Na and will be explored in more detail below. No increase in current at low concentrations of Ca, Mg, or Ba was observed, but values $<50 \mu\text{M}$ were not tested. Such an increase might be expected if the channel was occupied by more than one ion at a time and if there was a significant degree of interaction between these ions.

The concentration of divalent cation required to produce 50% of the maximal block ($K_{1/2}$) was determined by plotting the fractional block of conductance (defined as $[G_{\text{unblocked}} - G_{\text{blocked}}]/G_{\text{unblocked}}$) at ± 30 mV as a function of the divalent cation concentration and fitting with the Hill relation. While the values derived from the Hill equation have no theoretical significance, they do provide a basis for comparison with data from rod channels. Such a plot for calcium, derived from the data in Fig. 3 A is shown in Fig. 3 B. The mean $K_{1/2}$'s and Hill coefficients for Ca, Mg, and Ba are shown in Table I. The efficacy of block by these divalent cations at +30 mV ranked in the order $\text{Ca} > \text{Mg} > \text{Ba}$, whereas at -30 mV, the rank order was $\text{Ca} > \text{Ba} > \text{Mg}$. In all cases, the values for $K_{1/2}$ were lower at positive potentials than at negative potentials. In all cases except for Mg at +30 mV, the mean Hill coefficients were not significantly different from 1, suggesting that the binding of a single divalent cation may be sufficient to block the channel. For all of these ions, the values for $K_{1/2}$ were quite variable from patch to patch, even in the same prepa-

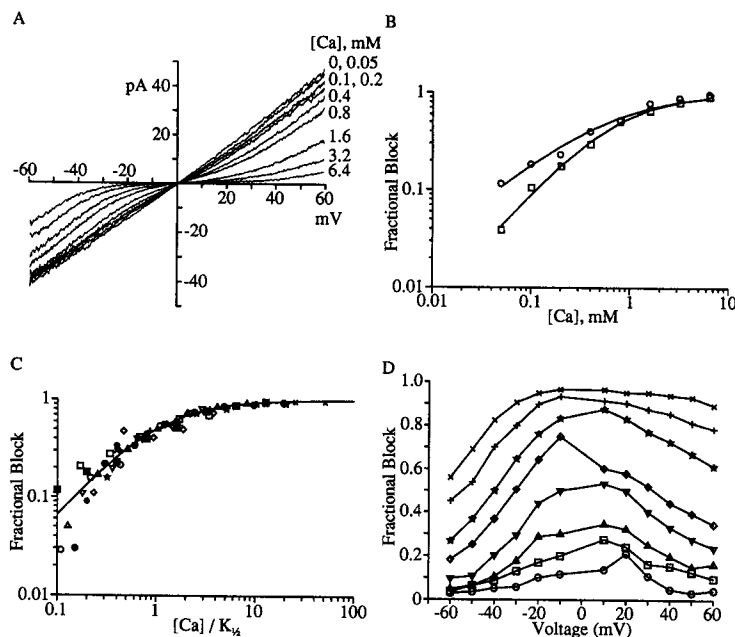


FIGURE 3. Block of sodium current by intracellular calcium. (A) Typical current-voltage relations showing block by calcium. 120 mM Na was present on both sides of the patch, with 0.05, 0.1, 0.2, 0.4, 0.8, 1.6, 3.2, or 6.4 mM Ca added on the cytoplasmic side of the patch. (B) Fractional block of the conductance by Ca at +30 mV (○) and -30 mV (□). The solid lines were derived from the Hill relation with apparent $K_{1/2}$'s and Hill coefficients of 630 μ M and 0.84 (+30 mV) and 747 μ M and 1.13 (-30 mV). Note that the values for the abscissa and $K_{1/2}$'s are in concentration rather than activity to facilitate comparison with previous work. (C) Fractional block of the current by Ca at +30 mV. Data from 11 different patches (different symbol for each patch). The concentration of Ca has been normalized by the value of $K_{1/2}$ in each experiment. The solid line is derived from the Hill relation with a $K_{1/2}$ of 1 and a Hill coefficient of 1.15 (the mean value). The shape of the curve was invariant with respect to $K_{1/2}$ and showed no deviation at low concentrations. (D) Fractional block as a function of voltage. Symbols: 0.05 (○), 0.1 (□), 0.2 (△), 0.4 (▽), 0.8 (◇), 1.6 (☆), 3.2 (+) and 6.4 (×) mM Ca. The lack of a monotonic relation indicates that calcium is a permeant blocker, not impermeant as required for a meaningful interpretation of δ in Woodhull's equation for fractional block.

ration. This degree of variability suggests the presence of inhomogeneity, possibly as a result of modulation of the channel by phosphorylation or other mechanisms. The shape of the fractional block relation was invariant regardless of the value of $K_{1/2}$ (Fig. 3 C), however.

For all three divalent cations tested, block by divalent cations from the cytoplasmic side of the channel was greater at positive potentials than at negative potentials, consistent with a blocking mechanism in which divalent cations enter and transiently block the pore. Block was never complete, regardless of how positive the potential became, consistent with the small but finite permeability of divalent cations through the channel. This can be clearly seen in Fig. 3 D where the fractional

TABLE I
Concentration-dependence of Block by Divalent Cations from the Intracellular Side

Ion	+30 mV		-30 mV		<i>n</i>
	<i>K</i> _{1/2}	<i>n</i> _H	<i>K</i> _{1/2}	<i>n</i> _H	
	μM		μM		
Ca	319 ± 154	1.15 ± 0.20	624 ± 231	1.11 ± 0.29	10
Mg	410 ± 107	1.24 ± 0.20*	1236 ± 351	0.98 ± 0.19	7
Ba	589 ± 145	0.96 ± 0.14	639 ± 107	1.05 ± 0.27	4

All values given as mean ± SD for the number of experiments (*n*). Dissociation constants (*K*_{1/2}) and Hill coefficients (*n*_H) from the Hill relation.

*Significantly different from 1.0 at *p* < 0.05.

block is plotted as a function of voltage. For an impermeant blocker, one would expect a monotonically increasing fractional block with depolarization, but this is clearly not the case. As a consequence of this, the fraction of the voltage drop crossed by a blocking ion to reach its binding site would be overestimated.

Block by Ca and Mg from the Extracellular Side

Under physiological conditions, the net current through these channels is inward and the channels are blocked by extracellular calcium and by intracellular and extracellular magnesium. The fact that patches from rods or cones fail to form in the outside-out configuration has, until now, precluded examination of block by extracellular divalent cations in excised patches where the composition of the solutions can be closely controlled. One way around this problem is to perfuse the interior of the pipette, replacing the original divalent-free solution with one containing magnesium or calcium.

Perfusion of the pipette presents several problems. First, only a single perfusate can be used (see Methods) and therefore the experiments were not reversible. Second, replacement of the pipette solution depends upon diffusion of the ions into and out of the tip of the electrode, which may be a slow and incomplete process. For this reason, 6.4 mM Ca or Mg was used since this concentration of these ions appears to maximally block the channel when applied to the intracellular side of the channel (Fig. 3). Current-voltage relations were obtained during the course of pipette perfusion, but were not used until the shift in the reversal potential was complete. Once the reversal potential was stable, current-voltage relations were obtained to determine the conductance ratios of blocked to unblocked current at ±30 mV.

The addition of 6.4 mM Ca to the extracellular side of the channel produced substantial block of the sodium current, together with a shift of the reversal potential from 0 mV towards more positive values (Fig. 4 A). This shift in reversal potential is consistent with a Ca/Na permeability ratio >1. In 19 determinations from 5 patches, the average reversal potential was 19.8 ± 3.9 mV. Using the mean reversal potential, Eq. 3 yields a permeability ratio of Ca to Na of 49.5. The mean conductance ratio (blocked/unblocked current) at +30 and -30 mV in these five patches was 0.036 ± 0.012 and 0.019 ± 0.010, respectively. The addition of 6.4 mM Ca to the

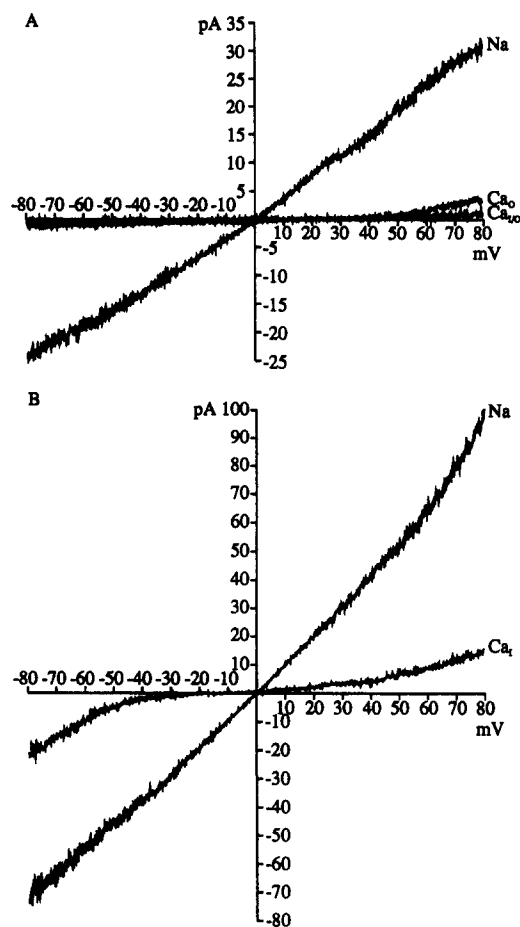


FIGURE 4. Block of sodium current by calcium. (A) Block by Ca from the extracellular side. The reversal potential was 0 mV at the beginning of the experiment with Ca-free 120 mM Na solution on both sides of the patch. The pipette solution was replaced by perfusion with 120 mM Na and 6.4 mM Ca (Ca_o), shifting the reversal potential to 17.4 mV and suppressing the conductance at ± 30 mV to 4.7 and 3.5%, respectively, of the unblocked conductance. Subsequent replacement of the bath solution with 120 mM Na and 6.4 mM Ca ($Ca_{i/o}$) shifted the reversal potential to 0 mV and further reduced the conductance at ± 30 mV to 1.7 and 2.3%, respectively. (B) Block by Ca from the intracellular side (Ca_i). Different patch from A. In this experiment, only the bath solution was replaced. The reversal potential shifted from 0 to -12.9 mV and the conductance at ± 30 mV was reduced to 8.2 and 0.6%, respectively, of the unblocked current.

cytoplasmic side of the patch as well as the extracellular side reduced the conductance ratio at $+30$ and -30 mV still further to 0.025 ± 0.016 and 0.022 ± 0.008 , respectively. The reversal potential under these symmetrical conditions returned to 0 mV.

To facilitate comparison, Fig. 4 B shows an experiment similar to that in Fig. 3 in which 6.4 mM Ca was added on only the intracellular side. As with addition of calcium on the extracellular side, this also produced a shift in the reversal potential but towards negative values and of lesser magnitude. In five patches, the mean reversal potential was -11.9 ± 2.9 mV. Using the mean reversal potential, Eq. 2 yields a permeability ratio of Ca to Na of 20.6, a factor of 4 lower than that obtained from the biionic sodium-calcium experiments in Fig. 2. Calcium at the intracellular side was also less effective at blocking sodium current than extracellular calcium. In seven patches, the conductance ratios at $+30$ and -30 mV were 0.058 ± 0.020 and 0.094 ± 0.037 , respectively. Not unexpectedly, the shape of the current-voltage relations for block from the two sides was different, indicating a degree of asymmetry within the channel.

Results similar to those of calcium were obtained with magnesium (Fig. 5). The addition of 6.4 mM Mg to the extracellular side of the channel shifted the reversal potential from 0 mV towards slightly more positive values (Fig. 5 A). In nine determinations from four patches, the average reversal potential was 5.2 ± 1.8 mV. Using the mean reversal potential, Eq. 3 yields a permeability ratio of Mg to Na of 6.6. The mean conductance ratio (blocked/unblocked current) at +30 and -30 mV in these four patches was 0.085 ± 0.067 and 0.062 ± 0.051 , respectively. The addition of 6.4 mM Mg to the cytoplasmic side of the patch as well as the extracellular side reduced the conductance ratio at +30 and -30 mV still further to 0.029 ± 0.016 and 0.028 ± 0.030 ($n = 2$), respectively, and returned the reversal potential to 0 mV.

The addition of 6.4 mM Mg on only the intracellular side (Fig. 5 B) shifted the reversal potential towards negative values. The magnitude of this shift was greater than for extracellular magnesium. In three patches, the mean reversal potential was -11.3 ± 5.1 mV. Using the mean reversal potential, Eq. 2 yields a permeability ratio of Mg to Na of 18.7, very similar to that obtained from the biionic sodium-magnesium experiments. Magnesium at the intracellular side is as effective a blocker of sodium current as extracellular magnesium. The conductance ratios at

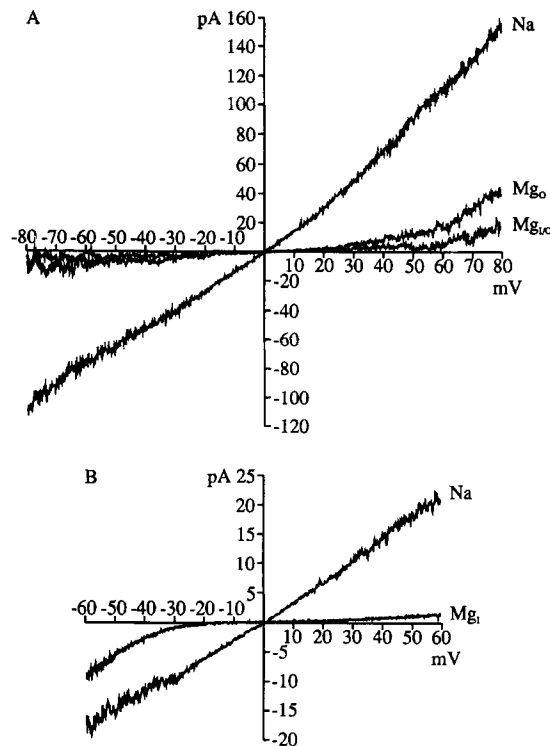


FIGURE 5. Block of sodium current by magnesium. (A) Block by Mg from the extracellular side. The reversal potential was 0 mV at the beginning of the experiment with Mg-free 120 mM Na solution on both sides of the patch. The pipette solution was replaced by perfusion with 120 mM Na and 6.4 mM Mg (Mg_o), shifting the reversal potential to +4 mV and suppressing the conductance at ± 30 mV to 13 and 11%, respectively, of the unblocked conductance. Subsequent replacement of the bath solution with 120 mM Na and 6.4 mM Mg ($Mg_{i/o}$) shifted the reversal potential to 0 mV and further reduced the conductance at ± 30 mV to 4.1 and 5%, respectively. (B) Block by Mg from the intracellular side (Mg_i). Different patch from A. In this experiment, only the bath solution was replaced. The reversal potential shifted from 0 to -13.5 mV and the conductance at ± 30 mV was reduced to 4 and 16%, respectively, of the unblocked current.

+30 and -30 mV were 0.055 ± 0.056 and 0.137 ± 0.036 , respectively. As with calcium, the shape of the current-voltage relations for block from the two sides were quite different, again indicating asymmetry within the channel.

DISCUSSION

Although there have been several studies of block by divalent cations of the rod channel (Colamartino et al., 1990; Zimmerman and Baylor, 1992; Tanaka and Furman, 1993), this is the first systematic investigation of permeation and block of the cone channel. Making a comparison with rods is difficult because the results obtained by various investigators differ from each other. The efficacy of block of the cone channel by divalent cations at positive potentials as found here are similar to those of Zimmerman and Baylor (1992) and Tanaka and Furman (1993) in the rod channel, who both found that $\text{Ca} > \text{Mg}$ (+30 and +80 mV, respectively), but are different from those of Colamartino et al. (1991) who found $\text{Mg} > \text{Ba} > \text{Ca}$ (+60 mV). At negative potentials, Zimmerman and Baylor (1992) and Tanaka and Furman (1993) both found $\text{Mg} > \text{Ca}$ (-30 and -80 mV, respectively) and Colamartino et al. (1991) found $\text{Ba} > \text{Ca} > \text{Mg}$, all of which are different from the results in cones ($\text{Ca} > \text{Ba} > \text{Mg}$). Thus, it would appear that the ability of divalent cations to block the channel from the intracellular side is similar in rods and cones at positive voltages, but different at the physiologically important negative voltages. The conditions used by Zimmerman and Baylor (1992) to study the rod channel were most similar to those used here. They found that calcium applied to the cytoplasmic face of the channel had an apparent dissociation constant of $\sim 400 \mu\text{M}$ at -30 mV and $\sim 1.4 \text{ mM}$ at +30 mV, as compared with $\sim 620 \mu\text{M}$ at -30 mV and $\sim 320 \mu\text{M}$ at +30 mV found here for the cone channel. Comparing their results with those presented here, two things are immediately apparent. The first is that the voltage dependence of the apparent dissociation constant is reversed and reduced in the cone channel as compared with the rod channel, and the second is that the cone has a lower affinity for calcium in the physiologically relevant voltage range near -30 mV. If this lower affinity holds true for externally applied calcium, then the lower affinity of the cone channel (which probably reflects a faster unbinding rate of the ion from its site) leads to the conclusion that the cone channel should have a higher influx of calcium relative to sodium than the rod channel since the time calcium spends bound to its site is reduced. This supports the findings of Perry and McNaughton (1991) that the fraction of inward current carried by calcium is higher in the cone than in the rod. Because the cone also has a smaller cytoplasmic volume than does the rod, this would lead to more rapid changes in the concentration of intracellular calcium (Nakatani and Yau, 1989).

One of the remarkable findings of the experiments presented here is the variability of the permeability ratios and of the apparent dissociation constants for block of the sodium current by divalent cations presented at the intracellular side of the channel. This is not true for monovalent cation permeability ratios (Haynes, 1995). In some sense, the intracellular side of the channel seems to be "fuzzy" in its properties with respect to divalent cations. One possibility is that modulation of the channel, perhaps by phosphorylation or some other mechanism, may predomi-

nantly affect the cytoplasmic side of the pore. This could represent a physiological mechanism whereby the ratio of Na to Ca in the dark current could be changed, possibly during light adaptation.

The question arises whether there is only a single binding site or multiple sites. For monovalent cations, permeation can be described by a single-site Eyring model. Multiple sites would be an immediate consequence of multiple occupancy of the channel. Multiple occupancy of the channel would be demonstrated by concentration-dependent permeability ratios, anomalous mole fraction behavior, conductance-concentration relations with multiple dissociation constants or blockers with values for δ (the apparent fraction of the membrane voltage crossed by a charged blocker to reach its binding site) exceeding 1. Anomalous mole fraction behavior between lithium and sodium has not been observed for the cone channel (Haynes, 1995), nor has it been observed for block by calcium. Tanaka and Furman (1993) observed an anomalous mole-fraction-like effect in the block of the rod channel by calcium. They concluded that there were two sites with very different affinities, the high affinity site outside the membrane voltage drop which affected gating and the low affinity site within the membrane voltage drop which blocked the channel. Thus, only single occupancy was required. The very low concentrations of divalent cations used by Tanaka and Furman (1993) were not used here because the small effect that they reported would be easily obscured by small variations in the seal resistance that typically occur in cone patches. In the experiments presented here, the concentration dependence of the fractional block by divalent cations showed only a single dissociation constant and in all cases except one (Mg at +30 mV), the mean Hill coefficients were not significantly different from 1. In preliminary experiments (Stotz and Haynes, 1995), impermeant organic cations block sodium current through the cone channel and give values for $\delta < 1$. These observations are consistent with single occupancy of the channel. It must be concluded that the failure of these experiments to show multiple occupancy of the cone channel do not rule out a multi-ion channel, but neither do they provide any evidence for multiple occupancy.

Eyring Rate Theory Models

In the previous paper (Haynes, 1995), I presented an Eyring model for monovalent cation permeation using two barriers and a single site. This model, with slight modifications, also provided an adequate fit to the divalent cation data. Significantly better fits were not obtained using a more complicated model consisting of three barriers and two binding sites. Three such two-site models were tested: a single-occupancy model, a double-occupancy model without ion-ion interaction and a double-occupancy model with ion-ion interaction. One assumption underlying these models is that change in current observed upon substituting or adding divalent cations is solely due to the permeation process rather than a reduction of the open probability of the channel. The addition of Ca^{2+} can, however, alter the open probability of the rod channel (Sesti, Straforini, Lamb, and Torre, 1994) via a calmodulin-dependent interaction (Hsu and Molday, 1993; Gordon, Downing-Park, and Zimmerman, 1994). However, such effects occur only at low concentrations of cGMP, not at the saturating concentrations used in this study, nor have they been

demonstrated in cone channels. Thus, it should be safe to assume that only permeation effects are being modeled.

The large degree of variability in the dissociation constants for block by calcium and magnesium and for their permeability ratios precluded fitting all of the data. Instead, a representative set of current-voltage relations at different concentrations of divalent cation obtained from a single patch and with dissociation constants near the mean values was selected. The current-voltage relations at 6.4 mM divalent cation concentration (intracellular, extracellular or both) were used from the remainder of the patches studied since this concentration is sufficient to very nearly saturate the block. A total of 511 data points for divalent cations, obtained by sampling the current-voltage relations at 10-mV increments, were used in the fitting process. These were added to the data set used in the previous paper (Haynes, 1995) for a total of 2,478 data points and all eight ions were fitted simultaneously.

Of the four models tested, the single-site, two-barrier model provided fits as good as the more complicated two-site, three-barrier models. Of the later, the single-occupancy model provided the best fit, followed by the multiple-occupancy without ion-ion interaction model. The multiple-occupancy model with ion-ion interaction converged to either 0 or infinite interaction energy, indicating that the data were insufficient to determine the energies of interaction (if any). The energy profile of the single-site model and the current-voltage relations that it predicts are shown in Fig. 6. The two barriers are located at ~ 29 and 94% of the way across the electric field drop from the cytoplasmic surface. The single binding site is located at $\sim 61\%$ across. The parameters for the energies of the barriers and binding sites for the various ions are given in Table II. The currents predicted by the model are all in reasonable agreement with those observed for block by Ca (Fig. 6, *C-E*) or Mg (Fig. 6, *F-H*). Moreover, the model predicts the shift in the reversal potential with increasing concentrations of Ca and predicts only a small shift for Mg, both in agreement with the observations. The model does, however, produce a less pronounced outward rectification than that observed under conditions of block by in-

TABLE II
Parameters for a Three-Barrier, Two-Site Eyring Model

Ion	Peak 1	Well 1	Peak 2
Li	5.96	-8.04	5.68
Na	6.57	-6.96	5.03
K	6.11	-7.02	5.47
Rb	6.50	-7.62	5.21
Cs	6.39	-7.87	6.05
NH ₄	5.49	-7.97	4.30
Ca	5.08	-14.72	2.33
Mg	6.27	-14.16	3.62
Distance	0.29	0.61	0.94

Surface charge (cytoplasmic side): 0.022 C m^{-2} . Surface charge (extracellular side): 0.0032 C m^{-2} . Energies in units of kT; distance is in fraction of the electric field drop (0 at cytoplasmic side). The conventions and standard state used here are those described by Alvarez et al. (1992).

tracellular divalent cations. Note that the current-voltage relations predicted for the monovalent cations are not shown, because they are indistinguishable from those shown in the previous paper (Haynes, 1995).

Having fitted the model to data from both mono- and divalent cations, it is now possible to calculate the individual components of the current under physiological conditions. The "physiological conditions" chosen were those of Haynes and Yau (1985) in their paper first describing the properties of the channel in excised patches. With an extracellular solution of (in millimolar) 110 NaCl, 2.5 KCl, 1.0 CaCl₂ and 1.6 MgCl₂ and an intracellular solution of 12.5 NaCl, 100 KCl, and 1.6 MgCl₂, the model predicts the current-voltage relation shown in Fig. 6 B. In this figure, the solid line is the prediction of the model, while the circles are derived from the data of Haynes and Yau (1985) scaled so that the currents at +40 mV are equal.

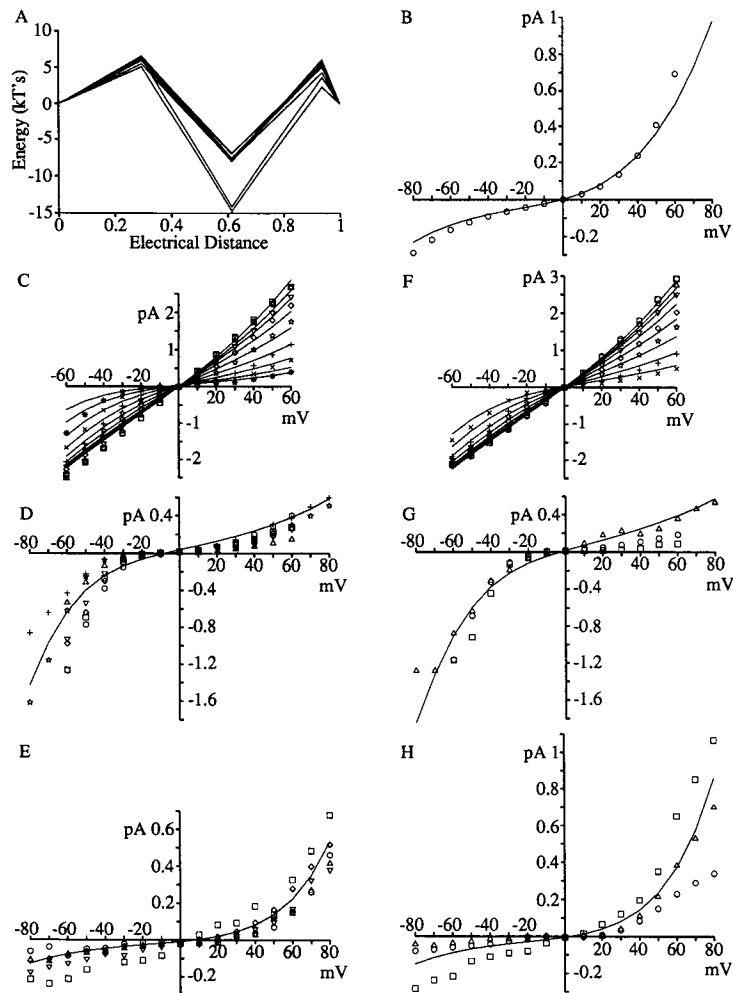


FIGURE 6.

The form of the current-voltage relation is in reasonable qualitative agreement with the experimental data in that the current increases exponentially at both positive and negative potentials. It is also in reasonable quantitative agreement. Although it predicts less current at strongly positive potentials than actually observed, it does a very good job at negative potentials. Haynes and Yau (1985) found a ratio of net currents at +40 and -40 mV of ~ 2.7 whereas the model predicts a ratio of ~ 2.9 . At -30 mV, the model predicts a net (inward) current of -60 fA, giving a conductance of 2 pS. The conductance of the rod channel as measured by noise analysis under similar conditions is ~ 0.1 pS (reviewed in Yau and Baylor, 1989), ~ 20 -fold lower. The net inward current at -30 mV is comprised of the net currents for each ion: -62 fA Na, -10 fA Ca, -4 fA Mg and +16 fA K. Of the -76 fA carried by the influx of cations, the ratio of $I_{\text{Na}}:I_{\text{Ca}}:I_{\text{Mg}}$ is 0.82:0.13:0.05. When measured as the fraction of the -60 fA net current, the proportion carried by Ca rises to 17%. This value is probably slightly underestimated because the model predicts less current than observed. It is, however, in reasonable agreement with the estimate of 21% obtained by Perry and McNaughton (1991) and higher than that in rods ($\sim 15\%$, Nakatani and Yau, 1988*b*). This, together with the higher conductance, further supports the idea that the rate of calcium influx into cones is higher than in rods. This larger influx of calcium into the smaller cytoplasmic volume of the cone coupled with the necessarily faster rate of efflux via the Na/Ca-K exchanger serves to make the rate of light adaptation in cones faster than in rods.

I wish to thank Maria J. Polyak for technical assistance. Thanks also to Drs. S. A. Barnes, R. J. French, and K. Hoehn for helpful discussion and critical reading of the manuscript.

This work was supported by the Alberta Heritage Foundation for Medical Research and the Medical Research Council of Canada.

Original version received 30 August 1994 and accepted version received 14 April 1995.

FIGURE 6. (*opposite*) Two-barrier, one-site Eyring model and predicted currents. (A) Schematic diagram of the model. The energy of each barrier and binding site are given in values of kT. The position of each peak or binding site is plotted as the fraction of the voltage drop crossed by an ion moving from the cytoplasmic side (0) to the extracellular side (1) of the channel. See Table II for the exact values. Each line represents a different ion. The tight grouping of the two sets of lines representing monovalent cations and divalent cations, respectively, reflects the similar behaviour of ions in each of these two classes. (B) Predicted current-voltage relation under physiological conditions with (in millimolar) 110 NaCl, 2.5 KCl, 1.6 MgCl₂, 1.0 CaCl₂ extracellularly and 12.5 NaCl, 100 KCl, 1.6 MgCl₂ intracellularly. The line shows the prediction of the model using the parameters obtained by fitting the data in *C-H*. The circles are derived from the data of Haynes and Yau (1985) and scaled to match the current predicted by the model at +40 mV. (C) Current-voltage relations predicted for block by 0 (○), 0.05 (□), 0.1 (△), 0.2 (▽), 0.4 (◇), 0.8 (☆), 1.6 (+), 3.2 (×) and 6.4 (*) mM internal Ca. (D) Block by internal 6.4 mM Ca. (E) Block by 6.4 mM external Ca. (F) Current-voltage relations predicted for block by 0 (○), 0.05 (□), 0.1 (△), 0.2 (▽), 0.4 (◇), 0.8 (☆), 1.6 (+) and 3.2 (×) mM internal Mg. (G) Block by internal 6.4 mM Mg. (H) Block by external 6.4 mM Mg. For C and F, each symbol represents a different concentration in the same patch; data in the two plots from different patches. For D, E, G, and H, each symbol represents data from a different patch.

REFERENCES

- Butler, J. N. 1968. The thermodynamic activity of calcium ion in sodium chloride-calcium chloride electrolytes. *Biophysical Journal*. 8:1426-1433.
- Colamartino, G., A. Menini, and V. Torre. 1991. Blockage and permeation of divalent cations through the cyclic GMP-activated channel from tiger salamander rods. *Journal of Physiology*. 440: 189-206.
- Fesenko, E. E., S. S. Kolesnikov, and A. L. Lyubarsky. 1985. Induction by cyclic GMP of cationic conductance in plasma membrane of retinal rod outer segment. *Nature*. 313:310-313.
- Furman, R. E., and J. C. Tanaka. 1990. Monovalent selectivity of the cyclic guanosine monophosphate-activated ion channel. *Journal of General Physiology*. 96:57-82.
- Gordon, S. E., J. Downing-Park, and A. L. Zimmerman. 1994. Modulation of the cGMP-gated ion channel in frog rods by calmodulin and an endogenous inhibitory factor. *Journal of Physiology*. In press.
- Haynes, L. W. 1991. Mono- and divalent inorganic cation selectivity of the cGMP-gated channel of catfish cone outer segments. *Journal of General Physiology*. 98:13a. (Abstr.)
- Haynes, L. W. 1993. Mono- and divalent cation selectivity of catfish cone outer segment cGMP-gated channels. *Biophysical Journal*. 64:A133. (Abstr.)
- Haynes, L. W. 1994. Asymmetry of the permeation pathway in catfish cone cGMP-gated channels. *Biophysical Journal*. 66:A355. (Abstr.)
- Haynes, L. W. 1995. Permeation of internal and external monovalent cations through the catfish cone photoreceptor cGMP-gated channel. *Journal of General Physiology*. 106:485-505.
- Haynes, L. W., A. R. Kay, and K.-W. Yau. 1986. Single cyclic GMP-activated channel activity in excised patches of rod outer segment membrane. *Nature*. 321:66-70.
- Haynes, L. W., and K.-W. Yau. 1985. Cyclic GMP-sensitive conductance in outer segment membrane of catfish cones. *Nature*. 317:61-64.
- Haynes, L. W., and K.-W. Yau. 1990a. Single-channel measurement from the cyclic GMP-activated conductance of catfish retinal cones. *Journal of Physiology*. 429:451-481.
- Haynes, L. W., and K.-W. Yau. 1990b. The cGMP-gated channels of rod and cone photoreceptors. In *Transduction in Biological Systems*. C. Hidalgo, J. Bacigalupo, E. Jaimovich, and J. Vergara, editors. Plenum Publishing Corp., NY. 47-58.
- Hille, B. 1992. *Ionic Channels of Excitable Membranes*, Second Edition. Sinauer Associates, Inc., Sunderland, MA.
- Hsu, Y.-T., and R. S. Molday. 1993. Modulation of the cGMP-gated channel of rod photoreceptor cells by calmodulin. *Nature*. 361:76-79.
- Koch, K.-W., and L. Stryer. 1988. Highly cooperative feedback control of retinal rod guanylate cyclase by calcium ions. *Nature*. 334:64-66.
- Lewis, C. A. 1979. Ion-concentration dependence of the reversal potential and the single channel conductance of ion channels at the frog neuromuscular junction. *Journal of Physiology*. 286:417-445.
- Matthews, H. R., R. L. W. Murphy, G. L. Fain, and T. D. Lamb. 1988. Photoreceptor light adaptation is mediated by cytoplasmic calcium concentration. *Nature*. 334:67-69.
- Menini, A. 1990. Currents carried by monovalent cations through cyclic GMP-activated channels in excised patches from salamander rods. *Journal of Physiology*. 424:167-185.
- Nakatani, K., and K.-W. Yau. 1988a. Calcium and light adaptation in retinal rods and cones. *Nature*. 334:69-71.
- Nakatani, K., and K.-W. Yau. 1988b. Calcium and magnesium fluxes across the plasma membrane of the rod outer segment. *Journal of Physiology*. 395:695-729.

- Nakatani, K., and K.-W. Yau. 1989. Sodium-dependent calcium extrusion and sensitivity regulation in retinal cones of the salamander. *Journal of Physiology*. 409:525–548.
- Perry, R. J., and P. A. McNaughton. 1991. Response properties of cones from the retina of the tiger salamander. *Journal of Physiology*. 433:561–587.
- Picones, A., and J. L. Korenbrot. 1992. Permeation and interaction of monovalent cations with the cGMP-gated channel of cone photoreceptors. *Journal of General Physiology*. 100:647–673.
- Pitzer, K. S., and G. Mayorga. 1973. Thermodynamics of electrolytes. II. Activity and osmotic coefficients for strong electrolytes with one or both ions univalent. *Journal of Physical Chemistry*. 77:2300–2308.
- Robinson, R. A., and R. H. Stokes. 1970. *Electrolyte Solutions. The Measurement and Interpretation of Conductance, Chemical Potential and Diffusion in Solutions of Simple Electrolytes*. Second edition (revised). Butterworths and Co., Ltd., London. 31–32.
- Sesti, F., M. Straforini, T. D. Lamb, and V. Torre. 1994. Gating, selectivity and blockage of single channels activated by cyclic GMP in retinal rods of the tiger salamander. *Journal of Physiology*. 474:203–222.
- Stotz, S. C., and L. W. Haynes. 1995. Block of cone cGMP-gated channels by internal organic cations. *Biophysical Journal*. 68:A386. (Abstr.)
- Tanaka, J. C., and R. E. Furman. 1993. Divalent effects on cGMP-activated currents in excised patches from amphibian photoreceptors. *Journal of Membrane Biology*. 131:245–256.
- Yau, K.-W., and L. W. Haynes. 1986. Effect of divalent cations on the macroscopic cGMP-activated current in excised rod membrane patches. *Biophysical Journal*. 49:33a. (Abstr.)
- Yau, K.-W., L. W. Haynes, and K. Nakatani. 1986. Roles of calcium and cyclic GMP in visual transduction. In *Control of Cellular Activity*. H. Ch. Lüttgau, editor. F. Fischer, Stuttgart, and Sinaur Associates, Inc., MA. 343–366.
- Woodhull, A. M. 1973. Ionic blockage of sodium channels in nerve. *Journal of General Physiology*. 61:687–708.
- Zimmerman, A., and D. A. Baylor. 1986. Cyclic GMP-sensitive conductance of retinal rods consists of aqueous pores. *Nature*. 321:70–72.
- Zimmerman, A., and D. A. Baylor. 1992. Cation interactions within the cyclic GMP-activated channel of retinal rods from the tiger salamander. *Journal of Physiology*. 449:759–783.